

# PeroMAS: A Multi-agent System of Perovskite Material Discovery

Yishu Wang<sup>1</sup>, Wei Liu<sup>1</sup>, Yifan Li<sup>2</sup>, Shengxiang Xu<sup>1</sup>, Xujie Yuan<sup>3</sup>, Ran Li<sup>4</sup>, Yuyu Luo<sup>4</sup>, Jia Zhu<sup>5</sup>, Shimin Di<sup>1</sup>, Min-Ling Zhang<sup>1</sup>, Guixiang Li<sup>2</sup>

<sup>1</sup>School of Computer Science and Engineering, Southeast University, Nanjing, China

<sup>2</sup>School of Materials Science and Engineering, Southeast University, Nanjing, China

<sup>3</sup>School of Artificial Intelligence, Sun Yat-Sen University, Zhuhai, China

<sup>4</sup>Information Hub, Hong Kong University of Science and Technology (Guangzhou), Guangzhou, China

<sup>5</sup>School of Computer Science and Engineering, Zhejiang Normal University, Jinhua, China

Correspondence to {shimin.di,guixiang.li}@seu.edu.cn

## Abstract

As a pioneer of the third-generation photovoltaic revolution, Perovskite Solar Cells (PSCs) are renowned for their superior optoelectronic performance and cost potential. The development process of PSCs is precise and complex, involving a series of closed-loop workflows such as literature retrieval, data integration, experimental design, and synthesis. However, existing AI perovskite approaches focus predominantly on discrete models, including material design, process optimization, and property prediction. These models fail to propagate physical constraints across the workflow, hindering end-to-end optimization. In this paper, we propose a multi-agent system for perovskite material discovery, named PeroMAS. We first encapsulated a series of perovskite-specific tools into Model Context Protocols (MCPs). By planning and invoking these tools, PeroMAS can design perovskite materials under multi-objective constraints, covering the entire process from literature retrieval and data extraction to property prediction and mechanism analysis. Furthermore, we construct an evaluation benchmark by perovskite human experts to assess this multi-agent system. Results demonstrate that, compared to single Large Language Model (LLM) or traditional search strategies, our system significantly enhances discovery efficiency. It successfully identified candidate materials satisfying multi-objective constraints. Notably, we verify PeroMAS's effectiveness in the physical world through real synthesis experiments.

## Keywords

Agentic AI, AI4Science, Perovskite Material, Multi-Agent System

## 1 Introduction

Global climate change and traditional energy crises have established the development of renewable energy as a central objective for sustainable development [10, 30]. Given that solar energy is the most abundant and accessible renewable resource, solar cells serve as a critical pillar for achieving carbon neutrality and ensuring energy security [15, 46]. A primary focus of photovoltaic technology is improving the power conversion efficiency (PCE), which measures the conversion of incident light power into output electrical power. Crystalline silicon materials, characterized by stable systems and mature device processing, currently support large-scale energy supplies with a PCE nearing 26%. However, the Shockley-Queisser limit restricts single-junction silicon solar cells to a theoretical maximum PCE of approximately 33% [72], leading to diminishing marginal returns in silicon-based research.

In contrast, perovskite solar cells (PSCs) [34, 75] offer high manufacturability and rapid performance improvements. Over the past decade, the PCE of PSCs has increased from an initial 3.8% to over 26%, exceeding 33% in tandem configurations. Specifically, tandem PSCs utilizing perovskite materials can achieve efficiencies as high as 45%, successfully exceeding the fundamental limits of crystalline silicon devices [37, 75, 88]. Despite these advantages, the large-scale application of PSCs remains hindered by severe challenges, including limited long-term stability [33, 86, 91], the toxicity of lead-based materials [32, 83], and poor reproducibility in scalable manufacturing [73]. Overcoming these challenges requires optimization of the perovskite material discovery process, including material compositions, lattice structure, and processing parameters [54].

Perovskite material discovery constitutes a multi-step scientific workflow defined by four core tasks: knowledge preparation, design, dry-lab, and wet-lab terminology [76]. Knowledge preparation serves as the research foundation, comprising literature retrieval, the aggregation of historical data, and the extraction of dispersed experimental parameters—such as A/B/X site occupancy, precursor concentration, spin-coating speed, and annealing temperature. These parameters, along with performance metrics (e.g., PCE,  $V_{oc}$ ,  $J_{sc}$ , and FF), are organized into structured databases [21]. Based on knowledge, researchers initiate material design by generating verifiable hypotheses [5, 49]. This process involves composition design [25], structural design [8], and process design [24] to formulate executable candidate solutions [49, 71]. To minimize prohibitive trial-and-error costs, dry-lab simulations are essential [63]. Specifically, density functional theory (DFT) calculations or machine learning (ML) models are employed to predict band structures, formation energies, and optoelectronic properties, enabling feasibility screening and providing necessary mechanistic analysis [41, 64]. Finally, wet-lab experiments represent the physical realization phase, encompassing synthesis, thin-film fabrication, device assembly, and rigorous performance testing and validation [85].

However, the discovery of novel perovskite materials using traditional trial-and-error methods remains inefficient. As shown in Figure 1, three primary artificial intelligence (AI) paradigms have been introduced to facilitate research on perovskite materials.

- **Machine Learning (ML):** Utilizing ML models such as Random Forest (RF) [90], Support Vector Machines (SVM) [14], and Graph Neural Networks (GNN) [77] to establish mappings between material structures or processing parameters and device performance. Leveraging the powerful fitting capability [7], ML

models enable the rapid prediction of properties, e.g., PCE, stability, and bandgap. For example, the GNoME project successfully predicted millions of stable crystal structures, including perovskites [18, 48]. Nevertheless, this paradigm generally supports only the automation of specific tasks, e.g., property prediction models fail to inform subsequent composition design directly. Furthermore, ML-based perovskite studies predominantly focus on single-objective optimization, typically maximizing PCE, rather than on multi-objective optimization [44, 80].

- **Large Language Model (LLM):** This paradigm involves pre-training or fine-tuning LLMs on perovskite literature to embed domain-specific knowledge. By leveraging advanced semantic understanding and generation capabilities, LLMs automate knowledge preparation, assisting diverse research tasks. For instance, Perovskite-LLM fine-tunes on 2,214 papers to support knowledge retrieval, literature reviews, experimental design, and complex problem-solving [38]. Similarly, Perovskite-R1 identifies high-quality small-molecule additives that are subsequently validated through wet-lab experiments [70]. Despite these advances, generative AI often underperforms on fundamental and specialized sub-tasks [57]. Especially, these approaches primarily internalizes knowledge into the model, failing to effectively leverage stable external tools to further extend their capabilities.
- **Multi-agents:** Built upon LLMs, multi-agent systems incorporate capabilities for planning, tool-use, reflection, and environmental interaction [87]. When integrated with self-driving laboratories, agents enable autonomous synthesis and characterization [4]. Their flexible task orchestration and global planning potential offer a pathway to resolve model fragmentation across the research workflow. For example, focusing exclusively on the single task of composition design, Lee et al. [31] proposed a multi-agent framework—comprising formula proposal, condition extraction, text gradient, and structure formatting agents—to discover novel double perovskites. However, this paradigm within the perovskite field remains insufficient, and a dedicated agent system covering the full process has not yet been developed.

As summarized in Figure 1, current AI-driven methods for perovskite material discovery either lack a single model to cover multiple tasks, or generative AI cannot guarantee that the generated content meets specific constraints for perovskite materials. Furthermore, most methods only focus on a single perovskite metric while ignoring other metrics, for example, optimizing PCE alone may compromise stability [39, 79].

To address above challenges, this paper presents the first specialized multi-agent system for perovskite material discovery. As illustrated in Figure 3, the system utilizes a hierarchical architecture with a *meta agent* and multiple *functional agents*. Meta agent is responsible for global task orchestration, constraint instantiation, and decision-making, ensuring workflow continuity across multiple tasks. To enhance task-solving capabilities, the system adopts a task-oriented approach, utilizing the Model Context Protocol (MCP) [19] to equip functional agents with specialized tools, including *miner agent*, *designer agent*, *emulator agent*, and *analyst agent*. Miner agent focuses on knowledge preparation, automating literature retrieval and data extraction to establish data priors

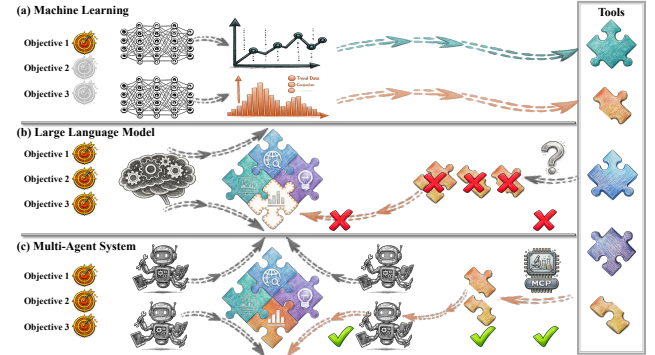


**Figure 1:** (a) Despite ML methods focus on single-objective mapping, they create high-precision specialized models that populate the PSC tool pool; (b) LLMs integrate domain knowledge for multi-objective tasks but may suffer from uncontrolled constraints and lack invocation for PSC tools; (c) We propose PeroMAS to orchestrate functional agents, which dynamically retrieving and utilizing tools from the PSC tool pool and achieving high-fidelity solutions.

as foundational hypotheses. Designer agent executes combinatorial design for compositions, structures, and processes, translating abstract hypotheses into concrete experimental parameters. Emulator agent is designed for dry-lab simulations where prediction models are automatically invoked to perform feasibility screening and multi-property forecasting. Analyst agent validates user requirements, performs attribution analysis on key factors, and provides recommendations to close the feedback loop for subsequent iterations. The primary contributions of this paper are as follows:

- We construct the first system in the perovskite domain that enables closed-loop iteration across knowledge preparation, design, and dry-lab simulation, effectively filling the research gap.
- By orchestrating functional agents via a Meta Agent and standardizing the integration of heterogeneous tools via the unified MCP interface, the system improves design outcomes under multi-objective constraints.
- We demonstrate the system’s practical reliability through a rigorous wet-lab experiment. Under high-efficiency and low-toxicity constraints, PeroMAS successfully identified a lead-reduced (50%) recipe that achieved a measured PCE of 17%, demonstrating high consistency with the system’s “dry-lab” predictions.
- We construct the first evaluation benchmark by perovskite human experts to assess PeroMAS. It includes an atomic-level dataset for subtasks and a full-task dataset containing complex multi-objective queries to facilitate research on agent planning and coordination.

## 2 Related Work

In the era of data-intensive science, AI not only accelerates research through large-scale processing and automation but also expands the boundaries of scientific discovery by extracting patterns and knowledge from complex datasets [69]. This section first

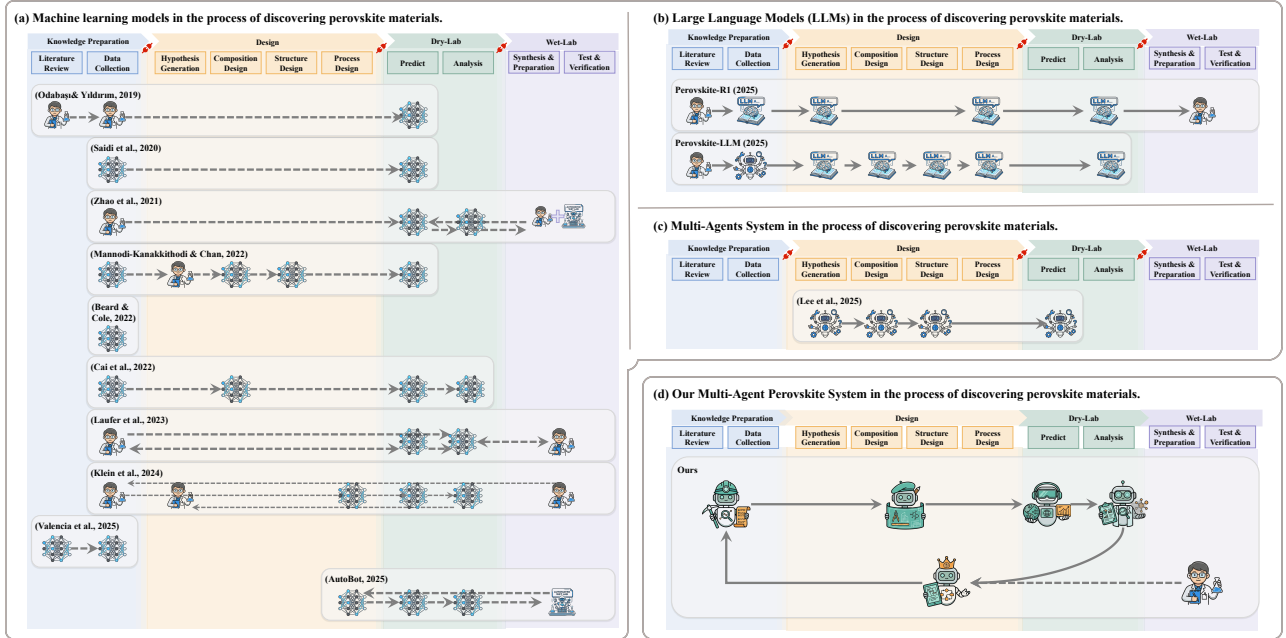


**Figure 2: A task-oriented overview of related work on AI for PSCs, including knowledge preparation, design, dry-lab, and wet-lab. PeroMAS automatically executes the full process for perovskite research and validates the candidates designed by PeroMAS through wet-lab experiments.**

reviews the progress of MAS across various scientific domains. Subsequently, we organize existing literature according to the core tasks of perovskite research.

## 2.1 Scientific Multi-Agent Systems

Multi-agent systems (MAS) can decompose complex scientific objectives into executable workflows in digital realm [52, 81]. In the physical realm, MAS can be coupled with robotic platforms to autonomously execute experiments. Together, these capabilities can reduce the burden on human researchers.

Coscientist represents a milestone in automated scientific research. This system develops a Planner responsible for high-level reasoning, task decomposition, and the scheduling of Web Searcher, Docs Searcher, Code Execution, and Automation Interface. It successfully accelerates chemical research across six tasks [4]. Furthermore, emerging research continuously facilitates automated research within the chemical domain. ChemAgents employs a task manager to coordinate literature mining, computational modeling, and robotic operations [59], while AutoLabs utilizes a graph-based architecture and self-check mechanisms to convert natural language instructions into validated, near-expert-level protocols for high-throughput liquid handlers [52].

In the biomedical domain, The Virtual Lab simulates a collaborative research team using hierarchical specialized agents and human feedback to reinforce scientific reasoning [62]. Similarly, CRISPR-GPT automates the gene-editing workflow validated by the Gene-editing Bench [55]. Furthermore, STELLA features a self-evolving mechanism that refines decision-making strategies to address novel biomedical challenges [26].

In the materials domain, SciAgents integrates large-scale ontological knowledge graphs with multi-agent systems, realizing

exploration capabilities that transcend human limits [13]. AtomAgents further integrates physics-aware reasoning with molecular simulations to address complex alloy design tasks through a collaborative multi-agent strategy [12].

MAS have similarly demonstrated potential in other scientific domains. PharmAgents simulates the complete drug discovery pipeline, from target discovery to preclinical evaluation [11], and PANGAEA GPT generates documentation for underutilized Earth system science datasets to drive further discovery [53]. Although these works validate the utility of MAS across various fields, the perovskite domain suffers from a lack of full-process MAS.

## 2.2 Artificial Intelligence for Perovskite

To accelerate perovskite research, artificial intelligence (AI) have been extensively explored across its multi-step workflow.

**Knowledge Preparation.** As the foundation of data-driven discovery, this stage faces the dual challenges of data scarcity and literature overload. While manual efforts like the Perovskite Database [21] provide structured high-quality data, they remain labor-intensive and prone to cognitive bias [61, 67]. Conversely, automated approaches, ranging from DFT calculations [1] and high-throughput experimentation [89] to LLM-based extraction [38, 66], offer scalability but often suffer from model obsolescence and irrelevant literature that can mislead task-specific decision-making.

**Prediction and Screening.** By learning the mapping between different material designs and their properties, machine learning (ML) models have successfully predicted key properties such as bandgaps, stability, and J-V characteristics [16, 56, 65]. These discriminative and predictive capabilities enable the rapid screening of vast chemical spaces, narrowing down thousands of candidates to a few promising candidates [5, 45]. However, these models are

primarily confined to attempting different combinations of known perovskite components, device structures, and processing conditions, rather than exploring unknown material designs.

**Analysis and Design.** To transcend simple property mapping, recent research integrates mechanistic analysis and generative design. While early ML and explainable AI methods identified statistical associations between fabrication parameters and performance [27, 29], lacking deep reasoning capabilities. Perovskite-LLM and Perovskite-R1 address this problem by synthesizing literature insights for knowledge retrieval and reasoning [38, 70]. Furthermore, Lee et al. [31] utilizes a surrogate-assisted agent framework to optimize double perovskite compositions. Nevertheless, these systems currently focus on single-task optimization, typically composition or processing, thereby neglecting the multi-objective interplay among composition, structure, and processing [9, 50].

**Wet Experimentation.** Finally, robotic platforms like RAPID and AURORA have demonstrated the potential for high-throughput synthesis and characterization, significantly compressing experimental cycles [36, 43]. However, fully autonomous discovery remains hindered by the heterogeneity of physical equipment and the inherent stochasticity of physical experiments, which sever the seamless interaction between digital and physical realms [6, 35, 47].

### 3 Methodology

This section presents our multi-agent framework for the autonomous discovery of perovskite materials. We first formalize the discovery task as a multi-objective optimization problem and outline the system architecture in Section 3.1. Section 3.2 details the Meta Agent, the system’s central orchestrator. Subsequently, Section 3.3 describes the four functional agents (Miner, Designer, Emulator, and Analyst), focusing on their tool execution via the Model Context Protocol (MCP) [19]. Finally, Section 3.4 validates the system through a standardized wet-lab synthesis procedure.

#### 3.1 Overview

Perovskite discovery faces two fundamental challenges: high-dimensional parameter coupling and conflicting multi-objective trade-offs (e.g., efficiency vs. stability) [48]. To address these, we formulate the discovery process as a dynamic optimization problem. Unlike existing machine learning approaches confined to isolated tasks [40, 79], we propose PeroMAS (Figure 3), a task-flow-oriented multi-agent system. It adopts a hierarchical architecture: a Meta Agent orchestrates central planning, while four functional agents (Miner, Designer, Emulator, Analyst) execute specialized subtasks using the Model Context Protocol (MCP) and shared memory, effectively resolving the fragmentation of traditional pipelines.

#### 3.2 Meta Agent

The Meta Agent serves as the system’s central reasoning unit, responsible for high-level task orchestration and global decision-making. Distinct from functional agents that rely on external tools, the Meta Agent operates as a logic-driven planner, translating user-defined objectives into an executable PDCA (Plan-Do-Check-Act) workflow. At the  $t$ -th iteration, it processes a composite state vector:

$$S_t = \{\mathcal{G}, \mathcal{M}, \mathcal{R}_{t-1}\}, \quad (1)$$

where  $\mathcal{G} = \langle O_{\text{obj}}, C_{\text{const}} \rangle$  encapsulates the multi-objective optimization targets and constraints;  $\mathcal{M}$  denotes the historical memory storing decision trajectories and execution logs; and  $\mathcal{R}_{t-1}$  represents the diagnostic feedback from the previous cycle.

Leveraging the Chain-of-Thought (CoT) mechanism [74], the Meta Agent executes a three-stage reasoning process:

- (1) **Goal Alignment:** It evaluates whether the feedback  $\mathcal{R}_{t-1}$  meets the termination criteria defined in  $\mathcal{G}$ . If targets are achieved or iteration limits reached, the process concludes.
- (2) **Reflection and Attribution:** For unfulfilled objectives, the agent analyzes  $\mathcal{M}$  to identify root causes of previous failures, ensuring the avoidance of proven ineffective paths.
- (3) **Strategy Formulation:** Based on the analysis, it instantiates abstract constraints into concrete scientific hypotheses  $\mathcal{H}_t$  and formulates the exploration strategy for the next iteration.

The reasoning outcome is formalized into a dynamic task orchestration instruction set  $\mathcal{P}_t$  for downstream agents:

$$\mathcal{P}_t = \{\mathcal{I}_{\text{Miner}}, \mathcal{I}_{\text{Designer}}, \mathcal{I}_{\text{Emulator}}, \mathcal{I}_{\text{Analyst}}\}. \quad (2)$$

These instructions define the contextual dependencies within the workflow. To optimize computational efficiency, the Meta Agent employs an adaptive pruning mechanism: by referencing  $\mathcal{M}$ , it identifies redundant sub-tasks (e.g., where valid data already exists) and sets their corresponding instructions to  $\emptyset$  (SKIP), thereby concentrating computational resources on unexplored design spaces.

#### 3.3 Function Agents

Guided by the Model Context Protocol (MCP) [19], four functional agents—Miner, Designer, Emulator, and Analyst—execute the closed-loop R&D process. These modules map to knowledge, design, prediction, and analysis phases, respectively. By ingesting upstream data and planning instructions, they ensure lossless context transmission while autonomously leveraging domain tools to generate concrete experimental results.

**3.3.1 Miner Agent.** Miner Agent is designed to address the “cold-start” challenge in the high-dimensional search space by constructing a domain knowledge base  $\mathcal{D}_{\text{obs}}$  from unstructured literature.

**Mechanism and Tool Integration:** The agent executes a two-stage “Retrieval-Extraction” workflow. First, it synthesizes the global goal  $\mathcal{G}$  and the current instruction  $\mathcal{I}_{\text{Miner}}$  into a retrieval query set  $\mathcal{Q}$ . By invoking the Literature Retrieval Interface (encapsulating APIs such as arXiv and ScienceDirect via MCP), it acquires a collection of highly relevant documents  $\mathcal{D}_{\text{doc}}$ . Subsequently, the agent utilizes a Semantic Extraction Toolchain—which synergizes domain-specific extraction models with LLMs [2, 68]—to construct an extraction function  $f_{\text{ext}}$ . This function parses unstructured texts  $d \in \mathcal{D}_{\text{doc}}$  into hybrid knowledge entries  $x_k$  containing design parameters ( $\mathcal{X}_{\text{design}}$ ), performance metrics ( $\mathcal{Y}_{\text{perf}}$ ), and mechanistic insights ( $\mathcal{S}_{\text{mech}}$ ):

$$x_k = f_{\text{ext}}(d \mid \mathcal{G}, \mathcal{I}_{\text{Miner}}) = \langle \mathcal{X}_{\text{design}}, \mathcal{Y}_{\text{perf}}, \mathcal{S}_{\text{mech}} \rangle. \quad (3)$$

Finally, the output dataset  $\mathcal{D}_{\text{obs}} = \{x_k\}_{k=1}^N$  is automatically merged into the system’s historical memory  $\mathcal{M}$ , providing the data foundation for downstream tasks.

**3.3.2 Designer Agent.** Designer Agent addresses the high-dimensional coupling challenge of composition, structure, and process ( $c, s, p$ ) by performing inverse design within the combinatorial space.

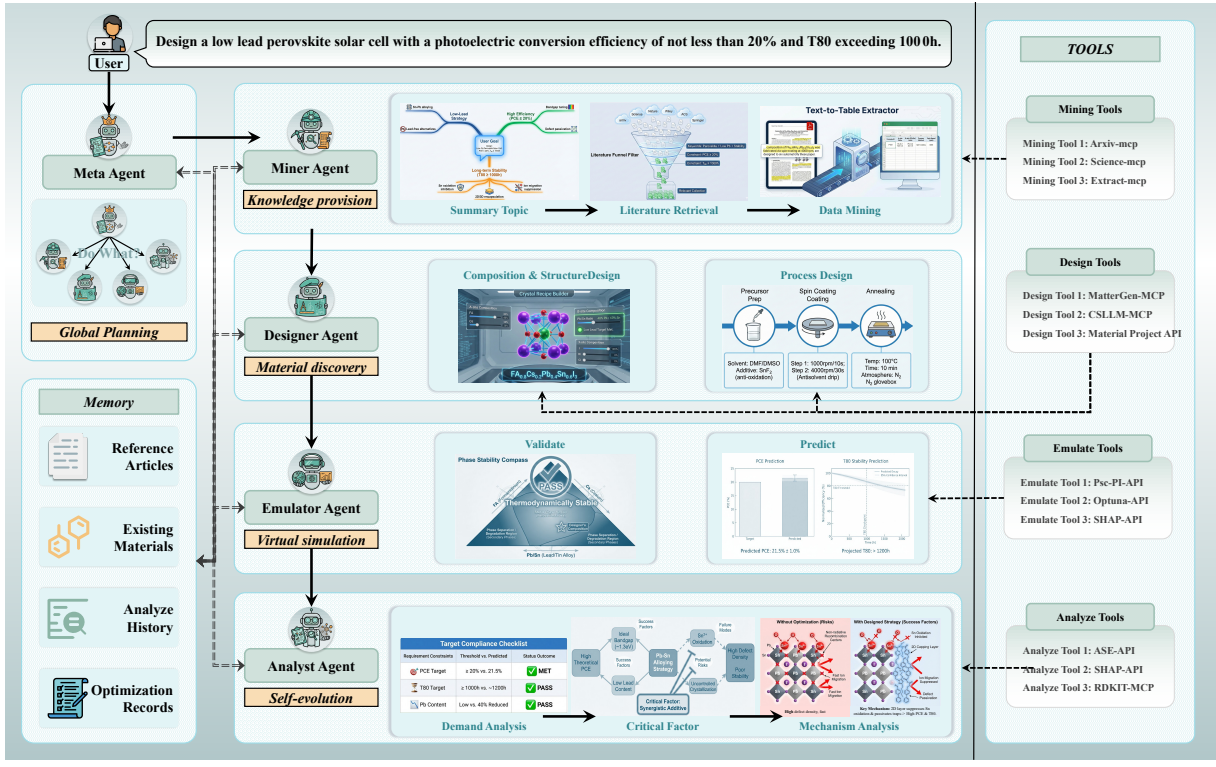


Figure 3: The system is centrally orchestrated by a Meta Agent responsible for global planning and memory management. It directs four functional agents, which are equipped with specialized domain tools via MCP to execute the closed-loop discovery workflow—spanning knowledge preparation, inverse design, property prediction, and mechanistic analysis.

**Mechanism and Tool Integration:** The agent employs a context-aware “Joint Generation-Constraint Filtering” mechanism driven by a “Generation-Reasoning” dual-engine toolchain. First, conditioning on the instruction  $I_{\text{Design}}$  and prior data  $\mathcal{D}_{\text{obs}}$ , it invokes the Material Generation Interface (integrating fine-tuned deep generative models [84]) to efficiently sample candidate compositions ( $c$ ) and structures ( $s$ ) from the latent space. Subsequently, a Synthesis-Aware LLM [60] complements these candidates by determining specific synthesis parameters ( $p$ ) and acting as a discriminator to filter out physically unfeasible proposals based on hard constraints  $g(x)$ . The joint generation process is formalized as:

$$x_{\text{cand}} = f_{\text{gen}}(I_{\text{Design}} \mid \mathcal{D}_{\text{obs}}) = \langle c, s, p \rangle. \quad (4)$$

The final output is a constraint-verified experimental proposal set  $X_{\text{new}} = \{x_i\}_{i=1}^K$ , then fed into the virtual screening phase.

**3.3.3 Emulator Agent.** Emulator Agent functions as a high-throughput virtual screening funnel to address the expensive, non-analytical black-box objective  $F(x)$  defined in the Overview.

**Mechanism and Tool Integration:** The agent employs a multi-dimensional property prediction workflow powered by a Heterogeneous Prediction Toolchain. Accepting the candidate set  $X_{\text{new}}$  from the Designer Agent and calibrating with prior data  $\mathcal{D}_{\text{obs}}$ , it parallelly invokes two core modules: the Graph Structure Prediction Interface (mounting Graph Neural Networks [78]) to predict intrinsic material properties (e.g., bandgap) from structure files, and the Machine Learning Regression Engine (integrating classic algorithms [20]) to infer device-level metrics like PCE and stability. Uniquely, the

agent outputs both point predictions  $\hat{y}_i$  and uncertainty estimates  $\sigma_i$  to quantify confidence. The result is an evaluated dataset  $X_{\text{eval}}$ , which identifies high-potential candidates maximizing the utility function  $U(\cdot)$ .

**3.3.4 Analyst Agent.** The Analyst Agent serves as the pivotal hub for the “Check” phase, synthesizing multidimensional data to diagnose performance discrepancies and close the discovery loop.

**Mechanism and Tool Integration:** The agent executes a two-layer “Rule Filtering-Attribution” pipeline. First, it aggregates the full data stream ( $\mathcal{D}_{\text{obs}}, X_{\text{new}}, X_{\text{eval}}$ ) and invokes the Material Rule Validator (encapsulating Pymatgen [51], ASE [17], and RDKit [28]) to conduct strict legality checks on stoichiometry and crystal structure, filtering out physically invalid candidates. Subsequently, for candidates failing to meet multi-objective targets, the Interpretable Inference Engine (based on SHAP analysis [42]) quantifies feature contributions to identify key constraints. The analysis is synthesized into an attribution diagnostic report  $\mathcal{R}$ , containing validity markers and mechanistic improvement strategies, which guides the Meta Agent in refining the hypothesis for the next iteration.

### 3.4 Wet-Lab Procedure

To ensure the physical viability of the material recipes and process parameters generated by PeroMAS, we collaborate with a professional experimental team in the perovskite field to establish a standardized fabrication workflow for perovskite solar cells (PSCs). This workflow employs a classic p-i-n inverted architecture [23],

effectively translating abstract AI design proposals into physical devices. The specific procedures are provided in Appendix C.

## 4 Experiments

### 4.1 Experimental Setup

**4.1.1 Training Datasets And Tool Calls.** We construct a full-chain MCP (Model Context Protocol) toolchain driven by real experimental data. We select The Perovskite Database [21] and execute a rigorous cleaning and completion process to obtain five-thousand pieces of full-dimensional “component-process-performance” data of perovskite in real scenarios. This data set forms the core knowledge base of the system and is directly used to train and fine-tune various specialized MCP tool models called by the agent.

**4.1.2 Evaluation Task Setup.** We designed a hierarchical evaluation protocol bridging “atomic execution” and “system-level decision-making” to comprehensively assess PeroMAS. This protocol will test the system from two dimensions: “single point task execution” to “full-process closed-loop decision-making”:

**Atomic Capability Evaluation.** We construct 130 specific tasks to strictly verify the execution accuracy of each individual agent.

- **Miner Task:** Evaluates the precision of literature retrieval and structured parameter extraction (composition, process, performance).
- **Designer Task:** Assesses the validity of inverse design proposals and the accuracy of physical feasibility judgments under hard constraints.
- **Emulator Task:** Tests the parallel processing capability for predicting key properties, specifically Power Conversion Efficiency (PCE) and Stability ( $T_{80}$ ).
- **Analyst Task:** Verifies the logic of feature attribution analysis and the scientific soundness of mechanism deduction reports.

**System-Level Evaluation** To evaluate collaborative problem-solving, we design 20 exploration tasks under conflicting multi-objective constraints (e.g., efficiency vs. stability vs. toxicity). This phase focuses on assessing the Meta Agent’s dynamic orchestration strategy and overall scientific rationality of the final experimental solutions.

**4.1.3 Baselines.** To benchmark our PeroMAS, we compare it against three representative paradigms ranging from tool-free inference to generalist autonomous agents:

**Standard LLM:** Uses the general-purpose gpt-4o for direct question answering without access to any external MCP tools or domain knowledge bases.

**Single ReAct Agent:** A monolithic agent (e.g. GPT-Agent) built on LangChain/AutoGPT [82] architectures. While equipped with MCP tool access, it processes tasks via a single linear ReAct loop, lacking the hierarchical planning capabilities of our system.

**Generalist Autonomous Agent:** The generalist frameworks like Manus [58]. We deploy it in the same perovskite environment to highlight the necessity of domain-specific architectural design over general-purpose autonomy.

**4.1.4 Evaluation Metrics.** To better quantify the results of the hierarchical evaluation protocol, we adopt two independent metric

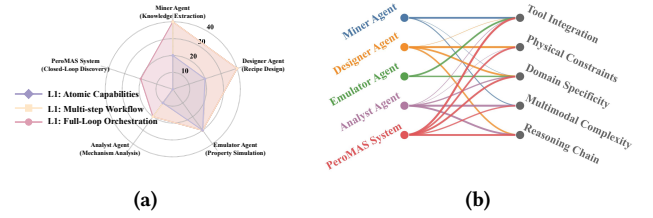


**Figure 4: Overview of PeroMAS-Bench dataset.** (a) Hierarchical task distribution across three complexity levels. (b) Capability contribution flow mapping agents to qualitative dimensions, where thickness indicates challenge intensity.

systems corresponding to the atomic capability evaluation of single agents and the full-loop evaluation of PeroMAS.

**Single-Agent Metrics** We assess atomic precision using three indicators: **Tool Accuracy (%)** evaluates execution correctness across two dimensions: Any-Order verifies the selection of the correct tool set, while Strict-Order enforces logical sequential execution consistent with the workflow. **Validity (0–10)** quantifies the scientific rationality of outputs, averaged from two sources: LLM-Score (assessing logical coherence via an independent evaluator) and Expert-Score (blinded peer review focusing on scientific value).

**System-Level Metrics** For complex multi-objective scenarios, **Task Completion (%)** measures the success rate of generating recipes that strictly satisfying constraints (e.g., efficiency, stability). **Output Validity (0–10)** evaluates the comprehensive quality of the final solution. Similar to single-agent metrics, this integrates automated assessments of report logic with professional expert evaluations regarding physical feasibility and potential impact.

**4.1.5 PeroMAS Benchmark.** We introduce PeroMAS-Bench, the first hierarchical evaluation dataset specifically designed for the perovskite domain. Constructed via the rigorous annotation pipeline detailed in Section 4.1.2, the benchmark comprises 150 high-fidelity evaluation instances that ensure comprehensive coverage of the research lifecycle. As shown in Figure 4a, the multi-layered architecture spans from foundational Miner tasks ( $N = 40$ ) for literature extraction to closed-loop discovery by PeroMAS ( $N = 20$ ).

To quantify dataset quality, we establish five cognitive dimensions: Tool Integration, Physical Constraints, Domain Specificity, Multimodal Complexity, and Reasoning Chain. As visualized in Figure 4b, the task-dimension binding is determined by the dominant capability required for valid execution: Miner tasks are rooted in Tool Integration for external retrieval, Designer tasks are bound by Physical Constraints to guarantee synthesizability, whereas Analyst tasks necessitate Multimodal Reasoning to interpret spectral data. All ground truth labels were verified by domain experts.

#### 4.1.6 Implementation Details.

**Backbone Models:** We benchmark PeroMAS across representative closed-source (GPT-4o, Claude-4.5, Gemini-2.5) and open-source (DeepSeek-V3, Qwen3) architectures. In each experimental group, all agents are uniformly instantiated with the same backbone model to ensure fair comparison.

**Hyperparameter Tuning:** Generation parameters are tailored to specific agent roles to balance precision and creativity:

**Table 1: Comparative evaluation of backbone models on core agent modules. Metrics include tool invocation accuracy (Any/Strict order) and output validity (0–10). Bold indicates the best result, and underlined denotes the second best.**

Agent Module	Core Capability	Metric	Backbone Model			
			GPT-4o	Claude-4.5	Gemini-2.5	DeepSeek-V3
Miner Agent	Knowledge Acquisition	Tool-Any-Order	<b>100.0%</b>	92.5%	<u>95.0%</u>	<u>95.0%</u>
		Tool-In-Order	<b>97.5%</b>	92.5%	<u>95.0%</u>	92.5%
		Validity (LLM)	<b>7.64</b>	<u>6.75</u>	5.17	6.46
		Validity (Expert)	<b>6.80</b>	5.80	4.80	<u>6.30</u>
Designer Agent	Composition & Recipe Design	Tool-Any-Order	76.6%	<b>93.3%</b>	83.3%	<u>86.6%</u>
		Tool-In-Order	73.3%	70.0%	<u>80.0%</u>	<b>83.3%</b>
		Validity (LLM)	6.74	<b>7.52</b>	5.62	<u>6.85</u>
		Validity (Expert)	6.40	<b>7.50</b>	<u>6.16</u>	5.50
Emulator Agent	Performance Predictive	Tool-Any-Order	<b>94.2%</b>	88.5%	90.2%	<b>100.0%</b>
		Tool-In-Order	<u>91.4%</u>	85.7%	88.5%	<b>97.1%</b>
		Validity (LLM)	<b>8.62</b>	8.26	8.05	<u>8.33</u>
		Validity (Expert)	<b>7.33</b>	<u>7.11</u>	6.56	6.56
Analyst Agent	Visual Analytics & Interpretability	Tool-Any-Order	90.0%	90.0%	90.0%	<b>95.0%</b>
		Tool-In-Order	75.0%	<b>90.0%</b>	80.0%	<u>85.0%</u>
		Validity (LLM)	<u>8.15</u>	7.76	<b>8.26</b>	7.65
		Validity (Expert)	<b>8.00</b>	<u>7.87</u>	7.62	<u>7.87</u>
Overall	System Average	<b>Avg. Tool Acc.</b>	84.3%	84.5%	<u>85.9%</u>	<b>89.5%</b>
		<b>Avg. Validity</b>	<b>7.13</b>	<u>7.07</u>	6.28	6.56

- Miner & Analyst ( $\tau = 0.1$ ): Prioritizes determinism to ensure precise data extraction and rigorous attribution logic.
- Designer ( $\tau = 0.7$ , Top- $p = 0.9$ ): Increases randomness to stimulate exploration within the vast material solution space.
- Meta Agent ( $\tau = 0.3$ ): Balances stability in global orchestration with flexibility in strategy adjustment.

**Automated Evaluation Setup:** We employ GPT-5.2 as the independent evaluator for validity metrics. To minimize variance, the evaluator temperature is locked at  $\tau = 0.1$ , following a strict double-blind protocol to assess both the planning trajectory and the final output.

**4.1.7 Wet-Lab Evaluation.** To evaluate the real-world feasibility of PeroMAS, we establish a discovery scenario under high-efficiency and low-toxicity constraints shown in Appendix B. Our experiments are conducted in a standardized perovskite device fabrication laboratory equipped with a full-chain fabrication and characterization platform, as shown in Figure 5a. All precursor preparation and thin-film deposition processes are carried out within nitrogen-filled gloveboxes to maintain a strictly inert atmosphere. We utilize a precision spin coater to execute the AI-generated spin-coating recipes, followed by electrode deposition via a high-vacuum thermal evaporation system. The final device performance is characterized under a standard AM 1.5G solar simulator. This high-specification experimental environment ensures a seamless translation from abstract AI strategies to physical realization.

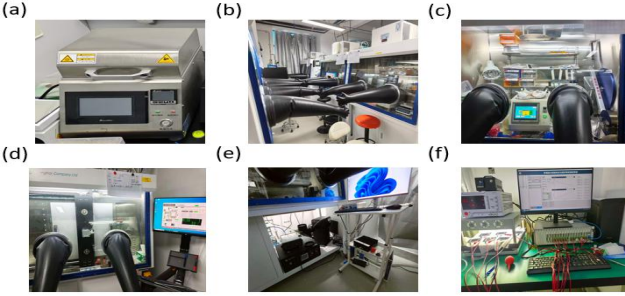
## 4.2 Results And Analysis

We will present a comprehensive analysis of the experimental results across five key dimensions: atomic performance, system-level performance, evaluation reliability, comparative benchmarking, and wet-lab validation of the generated proposals.

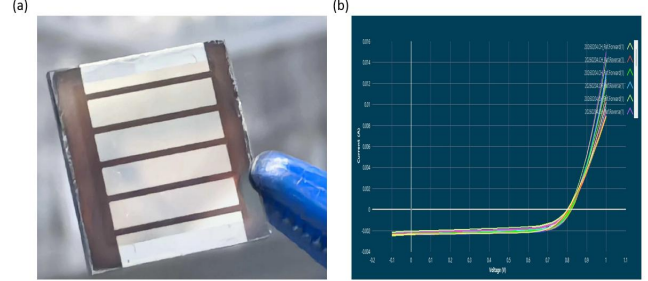
**4.2.1 Atomic Performance.** Table 1 highlights significant performance divergence across models. DeepSeek-V3 achieves a remarkable 89.5% tool accuracy, proving that open-source models can achieve functional parity with closed-source baselines in complex execution tasks. Claude-4.5 leads in overall output quality (Expert Score: 8.00) and complex recipe design, indicating that superior reasoning capabilities still demand the advanced cognitive depth of top-tier models.

**4.2.2 System-Level Performance.** Table 2 demonstrates that Claude-4.5 establishes the SOTA, achieving both the highest task completion (72.4%) and superior output validity (Expert Score: 7.14). Notably, the open-source DeepSeek-V3 outperforms GPT-5.2 specifically in Task Completion (61.8% vs. 59.0%). This confirms that while top-tier proprietary models dominate in scientific reasoning quality, well-orchestrated open-source agents can effectively bridge the execution gap in constrained tasks.

**4.2.3 Evaluation Consistency Analysis.** Figure 6a compares the score distributions between the LLM Judge and human experts. The two trajectories are highly congruent, with an average divergence of only  $\pm 0.15$  points across all models. This tight alignment



(a) Wet-Lab Procedure



(b) Wet-Lab Results

Figure 5: Practical validation of the PeroMAS system. (a) Used wet-lab devices for perovskite material synthesis. (b) Experimental results displaying the fabricated perovskite devices and their corresponding J-V curves for PCE evaluation.

Table 2: Performance evaluation of the fully autonomous perovskite material discovery workflow. **Bold** indicates the best performance, and underlined indicates the second best.

Base Model	Completion	Validity (LLM)	Validity (Expert)
GPT-5.2	59.0%	<u>6.52</u>	6.40
Gemini-2.5	48.7%	6.15	6.24
Claude-4.5	<b>72.4%</b>	<u>7.22</u>	<b>7.14</b>
DeepSeek-V3	61.8%	6.35	6.59
Qwen3	52.6%	6.05	5.92

confirms that, under rigorous scoring rubrics, GPT-5.2 model provides objective assessments highly consistent with expert judgment, thereby validating the reliability of our evaluation framework.

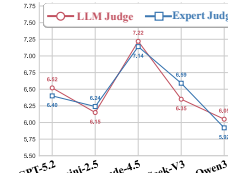
**4.2.4 Baseline Comparison Analysis.** To justify the necessity of a multi-agent architecture for perovskite discovery, we compare PeroMAS against three different paradigms, as shown in Figure 6b. The results yield three key architectural insights:

**Necessity of External Tools:** The Standard LLM (GPT-4o) scores lowest (5.90), confirming that internal parametric knowledge is insufficient for complex discovery. Integrating external MCP toolchains is a fundamental prerequisite for advanced scientific research.

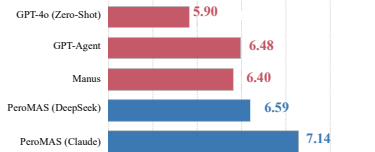
**Superiority of Domain Adaptation:** The generalist agent Manus underperforms the domain-specialized GPT-Agent. This reveals the limitations of "general-purpose autonomy" in niche scientific fields, which indicates that equip agents with domain-specific tools yields greater value than generalist agents.

**Collaborative Architecture Advantage:** Using identical tools, PeroMAS achieves a 10.2% performance gain over the single-agent baseline, validating that hierarchical task decomposition effectively reduces cognitive load. Notably, PeroMAS (DeepSeek-V3) outperforms proprietary baselines (Manus, GPT-Agent), suggesting that a superior collaborative framework outweighs raw model scale in multi-objective scientific challenges.

**4.2.5 Wet-Lab Results.** We select the Top-1 perovskite recipe generated by PeroMAS shown in Figure 8 for physical synthesis and performance characterization. This recipe employs a narrow-bandgap Sn-Pb mixed system that halves the lead content compared to



(a) Alignment



(b) Baseline Comparison

Figure 6: Evaluation consistency and performance benchmarking. (a) Alignment of score distributions between LLM Judge and human experts. (b) Performance comparison of PeroMAS against representative baselines across diverse agentic paradigms.

conventional pure-Pb counterparts, featuring a self-designed dual-additive combination of  $\text{SnF}_2$  and  $\text{EDAI}_2$ . Following the comprehensive fabrication protocol provided by PeroMAS, we successfully synthesize high-quality thin films and record a PCE of 17% via J-V characteristic testing in Figure 5b. This empirical performance falls strictly within the system's predicted range of 16%–19%, demonstrating exceptional consistency between the dry-lab simulation and physical realization.

## 5 Conclusion

We present PeroMAS, a hierarchical multi-agent framework that orchestrates the full digital R&D lifecycle of perovskites. By integrating the MCP, PeroMAS resolves the fragmentation of single-task models. Extensive evaluations demonstrate that our architecture significantly outperforms generalist agents, with open-source backbones (e.g., DeepSeek-V3) achieving parity with proprietary models. Notably, independent wet-lab validation confirmed a 17% PCE for an AI-designed Sn-Pb recipe, verifying the system's practical viability. With the release of the PeroMAS Benchmark, we provide a standardized foundation for the community, paving the way for future autonomous self-driving laboratories.

## References

[1] Edward J Beard and Jacqueline M Cole. 2022. Perovskite-and dye-sensitized solar-cell device databases auto-generated using chemdataextractor. *Scientific Data* 9, 1 (2022), 329.

[2] Iz Beltagy, Kyle Lo, and Arman Cohan. 2019. SciBERT: A Pretrained Language Model for Scientific Text. In *Proceedings of the 2019 Conference on Empirical Methods in Natural Language Processing and the 9th International Joint Conference on Natural Language Processing (EMNLP-IJCNLP)*, Kentaro Inui, Jing Jiang, Vincent Ng, and Xiaojun Wan (Eds.). Association for Computational Linguistics, Hong Kong, China, 3615–3620. doi:10.18653/v1/D19-1371

[3] Iz Beltagy, Kyle Lo, and Arman Cohan. 2019. SciBERT: A pretrained language model for scientific text. *arXiv preprint arXiv:1903.10676* (2019).

[4] Daniil A Boiko, Robert MacKnight, Ben Kline, and Gabe Gomes. 2023. Autonomous chemical research with large language models. *Nature* 624, 7992 (2023), 570–578.

[5] Xia Cai, Yiming Zhang, Zejiao Shi, Ying Chen, Yujie Xia, Anran Yu, Yuanfeng Xu, Fengxian Xie, Hezhu Shao, Heyuan Zhu, et al. 2022. Discovery of lead-free perovskites for high-performance solar cells via machine learning: ultrabroadband absorption, low radiative combination, and enhanced thermal conductivities. *Advanced Science* 9, 4 (2022), 2103648.

[6] Richard B Canty, Jeffrey A Bennett, Keith A Brown, Tonio Buonassisi, Sergei V Kalinin, John R Kitchin, Benji Maruyama, Robert G Moore, Joshua Schrier, Martin Seifrid, et al. 2025. Science acceleration and accessibility with self-driving labs. *Nature Communications* 16, 1 (2025), 3856.

[7] Rohan Chabra, Jan E Lenssen, Eddy Ilg, Tanner Schmidt, Julian Straub, Steven Lovegrove, and Richard Newcombe. 2020. Deep local shapes: Learning local sdf priors for detailed 3d reconstruction. In *European Conference on Computer Vision*. Springer, 608–625.

[8] Yimu Chen, Yusheng Lei, Yuheng Li, Yugang Yu, Jinze Cai, Ming-Hui Chiu, Rahul Rao, Yue Gu, Chunfeng Wang, Woojin Choi, et al. 2020. Strain engineering and epitaxial stabilization of halide perovskites. *Nature* 577, 7789 (2020), 209–215.

[9] Juan-Pablo Correa-Baena, Michael Saliba, Tonio Buonassisi, Michael Grätzel, Antonio Abate, Wolfgang Tress, and Anders Hagfeldt. 2017. Promises and challenges of perovskite solar cells. *Science* 358, 6364 (2017), 739–744.

[10] Haris Doukas and Alexandros Nikas. 2022. Europe’s energy crisis–climate community must speak up. *Nature* 608, 7923 (2022), 472–472.

[11] Bowen Gao, Yanwen Huang, Yiqiao Liu, Wenxuan Xie, Wei-Ying Ma, Ya-Qin Zhang, and Yanyan Lan. 2025. Pharmagents: Building a virtual pharma with large language model agents. *arXiv preprint arXiv:2503.22164* (2025).

[12] Alireza Ghafarollahi and Markus J Buehler. 2024. AtomAgents: Alloy design and discovery through physics-aware multi-modal multi-agent artificial intelligence. *arXiv preprint arXiv:2407.10022* (2024).

[13] Alireza Ghafarollahi and Markus J Buehler. 2025. SciAgents: automating scientific discovery through bioinspired multi-agent intelligent graph reasoning. *Advanced Materials* 37, 22 (2025), 2413523.

[14] Mehmet G’onen and Ethem Alpaydin. 2011. Multiple kernel learning algorithms. *The Journal of Machine Learning Research* 12 (2011), 2211–2268.

[15] Nancy M Haegel, Robert Margolis, Tonio Buonassisi, David Feldman, Armin Froitzheim, Raffi Garabedian, Martin Green, Stefan Glunz, Hans-Martin Henning, Burkhard Holder, et al. 2017. Terawatt-scale photovoltaics: Trajectories and challenges. *Science* 356, 6334 (2017), 141–143.

[16] Noor Titan Putri Hartono, Hans K’obler, Paolo Graniero, Mark Khenkin, Rutger Schlatmann, Carolin Ulbrich, and Antonio Abate. 2023. Stability follows efficiency based on the analysis of a large perovskite solar cells ageing dataset. *Nature Communications* 14, 1 (2023), 4869.

[17] Ask Hjorth Larsen, Jens Jørgen Mortensen, Jakob Blomqvist, Ivano E Castelli, Rune Christensen, Marcin Dulak, Jesper Friis, Michael N Groves, Bjørk Hammer, Cory Hargus, et al. 2017. The atomic simulation environment—a Python library for working with atoms. *Journal of Physics: Condensed Matter* 29, 27 (2017), 273002.

[18] Kurt Hornik, Maxwell Stinchcombe, and Halbert White. 1989. Multilayer feed-forward networks are universal approximators. *Neural networks* 2, 5 (1989), 359–366.

[19] Xinyi Hou, Yanjie Zhao, Shenao Wang, and Haoyu Wang. 2025. Model context protocol (mcp): Landscape, security threats, and future research directions. *arXiv preprint arXiv:2503.23278* (2025).

[20] Jinghao Hu, Zhengxin Chen, Yuzhi Chen, Hongyu Liu, Wenhao Li, Yanan Wang, Lin Peng, Xiaolin Liu, Jia Lin, Xianfeng Chen, et al. 2024. Interpretable machine learning predictions for efficient perovskite solar cell development. *Solar Energy Materials and Solar Cells* 271 (2024), 112826.

[21] T Jesper Jacobsson, Adam Hultqvist, Alberto Garc’ia-Fern’andez, Aman Anand, Amran Al-Ashouri, Anders Hagfeldt, Andrea Crovetto, Antonio Abate, Antonio Gaetano Ricciardulli, Anuja Vijayan, et al. 2022. An open-access database and analysis tool for perovskite solar cells based on the FAIR data principles. *Nature Energy* 7, 1 (2022), 107–115.

[22] Anubhav Jain, Shyue Ping Ong, Geoffroy Hautier, Wei Chen, William Davidson Richards, Stephen Dacek, Shreyas Cholia, Dan Gunter, David Skinner, Gerbrand Ceder, et al. 2013. Commentary: The Materials Project: A materials genome approach to accelerating materials innovation. *APL materials* 1, 1 (2013).

[23] Jun-Yuan Jeng, Kuo-Cheng Chen, Tsung-Yu Chiang, Pei-Ying Lin, Tzungs-Da Tsai, Yun-Chorng Chang, Tzungs-Fang Guo, Peter Chen, Ten-Chin Wen, and Yao-Jane Hsu. 2014. Nickel oxide electrode interlayer in CH3 NH3 PbI3 perovskite/PCBM planar-heterojunction hybrid solar cells. *Advanced Materials (Deerfield Beach, Fla.)* 26, 24 (2014), 4107–4113.

[24] Nam Joong Jeon, Jun Hong Noh, Young Chan Kim, Woon Seok Yang, Seungchan Ryu, and Sang Il Seok. 2014. Solvent engineering for high-performance inorganic–organic hybrid perovskite solar cells. *Nature materials* 13, 9 (2014), 897–903.

[25] Nam Joong Jeon, Jun Hong Noh, Woon Seok Yang, Young Chan Kim, Seungchan Ryu, Jangwon Seo, and Sang Il Seok. 2015. Compositional engineering of perovskite materials for high-performance solar cells. *Nature* 517, 7535 (2015), 476–480.

[26] Ruofan Jin, Zaixi Zhang, Mengdi Wang, and Le Cong. 2025. STELLA: Self-Evolving LLM Agent for Biomedical Research. *arXiv preprint arXiv:2507.02004* (2025).

[27] Lukas Klein, Sebastian Ziegler, Felix Laufer, Charlotte Debus, Markus G’otz, Klaus Maier-Hein, Ulrich W Paetzold, Fabian Isensee, and Paul F J’ager. 2024. Discovering process dynamics for scalable perovskite solar cell manufacturing with explainable AI. *Advanced Materials* 36, 7 (2024), 2307160.

[28] Greg Landrum. 2023. RDKit: Open-source chemoinformatics software. <https://github.com/rdkit/rdkit>

[29] Felix Laufer, Sebastian Ziegler, Fabian Schackmar, Edwin A Moreno Viteri, Markus G’otz, Charlotte Debus, Fabian Isensee, and Ulrich W Paetzold. 2023. Process Insights into Perovskite Thin-Film Photovoltaics from Machine Learning with In Situ Luminescence Data. *Solar RRL* 7, 7 (2023), 2201114.

[30] Dasom Lee. 2025. Meeting the energy challenge posed by data centres is central to a green future. *Nature* 639, 8055 (2025), S33–S33.

[31] Inhyo Lee, Junhyeong Lee, Jongwon Park, KyungTae Lim, and Seunghwa Ryu. 2025. Enhanced Conditional Generation of Double Perovskite by Knowledge-Guided Language Model Feedback. *arXiv preprint arXiv:2511.22307* (2025).

[32] Guixiang Li, Yong-Tao Liu, Feng Yang, Meng Li, Zuhong Zhang, Jorge Pascual, Zhao-Kui Wang, Shi-Zhe Wei, Xin-Yuan Zhao, Hai-Rui Liu, et al. 2024. Biotoxicity of halide perovskites in mice. *Advanced Materials* 36, 2 (2024), 2306860.

[33] Guixiang Li, Zhenhuang Su, Laura Canil, Declan Hughes, Mahmoud H Aldamasy, Janardan Dagar, Sergei Trofimov, Luyao Wang, Weiwei Zuo, José J Jerónimo-Rendon, et al. 2023. Highly efficient pin perovskite solar cells that endure temperature variations. *Science* 379, 6630 (2023), 399–403.

[34] Guixiang Li, Zuhong Zhang, Benjamin Agyei-Tuffour, Luyan Wu, Thomas W Gries, Karunanantharajah Prashanthan, Artem Musienko, Jinchao Li, Rui Zhu, Lucy JF Hart, et al. 2025. Stabilizing high-efficiency perovskite solar cells via strategic interfacial contact engineering. *Nature Photonics* (2025), 1–8.

[35] Xinyang Li, Yixin Li, Yiliang Zhou, Jiamin Wu, Zhifeng Zhao, Jiaqi Fan, Fei Deng, Zhaofu Wu, Guihua Xiao, Jing He, et al. 2023. Real-time denoising enables high-sensitivity fluorescence time-lapse imaging beyond the shot-noise limit. *Nature biotechnology* 41, 2 (2023), 282–292.

[36] Zhi Li, Mansoori Ani Najeeb, Liana Alves, Alyssa Sherman, Peter Cruz Parrilla, Ian M Pendleton, Matthias Zeller, Joshua Schrier, Alexander J Norquist, and Emory Chan. 2019. Robot-accelerated perovskite investigation and discovery (RAPID): 1. Inverse temperature crystallization. (2019).

[37] Jiang Liu, Yongcui He, Lei Ding, Hua Zhang, Qiaoyan Li, Lingbo Jia, Jia Yu, Ting Wai Lau, Minghui Li, Yuan Qin, et al. 2024. Perovskite/silicon tandem solar cells with bilayer interface passivation. *Nature* 635, 8039 (2024), 596–603.

[38] Xiang Liu, Penglai Sun, Shuyan Chen, Longhan Zhang, Peijie Dong, Huajie You, Yongqi Zhang, Chang Yan, Xiaowen Chu, and Tong-yi Zhang. 2025. Perovskite-llm: Knowledge-enhanced large language models for perovskite solar cell research. *arXiv preprint arXiv:2502.12669* (2025).

[39] Yingming Liu, Ziyang Zhang, Tianhao Wu, Wenxiang Xiang, Zhenzhen Qin, Xiangqian Shen, Yong Peng, Wenzhong Shen, Yongfang Li, and Liyuan Han. 2025. Cost Effectivities Analysis of Perovskite Solar Cells: Will it Outperform Crystalline Silicon Ones? *Nano-Micro Letters* 17, 1 (2025), 219.

[40] Andre Low, Yee-Fun Lim, Kedar Hippalgaonkar, and Eleonore Vissol-Gaudin. 2022. Mapping pareto fronts for efficient multi-objective materials discovery. *Authorea Preprints* (2022).

[41] Shuaihua Lu, Qionghua Zhou, Yixin Ouyang, Yili Guo, Qiang Li, and Jinlan Wang. 2018. Accelerated discovery of stable lead-free hybrid organic-inorganic perovskites via machine learning. *Nature communications* 9, 1 (2018), 3405.

[42] Scott M Lundberg and Su-In Lee. 2017. A unified approach to interpreting model predictions. *Advances in neural information processing systems* 30 (2017).

[43] Benjamin P MacLeod, Fraser GL Parlante, Thomas D Morrissey, Florian Häse, Loïc M Roch, Kevan E Dettelbach, Raphaell Moreira, Lars PE Yunker, Michael B Rooney, Joseph R Deeth, et al. 2020. Self-driving laboratory for accelerated discovery of thin-film materials. *Science Advances* 6, 20 (2020), eaaz8867.

[44] Benjamin P MacLeod, Fraser GL Parlante, Connor C Rupnow, Kevan E Dettelbach, Michael S Elliott, Thomas D Morrissey, Ted H Haley, Oleksii Proskurin, Michael B Rooney, Nina Taherimakhsousi, et al. 2022. A self-driving laboratory advances the Pareto front for material properties. *Nature communications* 13, 1 (2022), 995.

[45] Arun Mannodi-Kanakkithodi and Maria KY Chan. 2022. Data-driven design of novel halide perovskite alloys. *Energy & Environmental Science* 15, 5 (2022), 1930–1949.

[46] Ling Mao and Changying Xiang. 2025. A comprehensive review of machine learning applications in perovskite solar cells: Materials discovery, device performance, process optimization and systems integration. *Materials Today Energy* 47 (2025), 101742.

[47] S Hessam M Mehr, Matthew Craven, Artem I Leonov, Graham Keenan, and Leroy Cronin. 2020. A universal system for digitization and automatic execution of the chemical synthesis literature. *Science* 370, 6512 (2020), 101–108.

[48] Amil Merchant, Simon Batzner, Samuel S Schoenholz, Muratahan Aykol, Gowoon Cheon, and Ekin Dogus Cubuk. 2023. Scaling deep learning for materials discovery. *Nature* 624, 7990 (2023), 80–85.

[49] Pavel Nikolaev, Daylond Hooper, Frederick Webber, Rahul Rao, Kevin Decker, Michael Krein, Jason Poleski, Rick Barto, and Benji Maruyama. 2016. Autonomy in materials research: a case study in carbon nanotube growth. *npj Computational Materials* 2, 1 (2016), 1–6.

[50] Donghyun Oh, Sanggyun Kim, Carlo AR Perini, Juan-Pablo Correa-Baena, and Nikolaos V Sahinidis. 2025. Algorithm-Guided Experimentation for Optimization of High-Performance Perovskite Solar Cells. *ACS Energy Letters* 10, 12 (2025), 6037–6046.

[51] Shyue Ping Ong, William Davidson Richards, Anubhav Jain, Geoffroy Hautier, Michael Kocher, Shreyas Cholia, Dan Gunter, Vincent L Chevrier, Kristin A Persson, and Gerbrand Ceder. 2013. Python Materials Genomics (pymatgen): A robust, open-source python library for materials analysis. *Computational Materials Science* 68 (2013), 314–319.

[52] Gihan Panapitiya, Emily Saldanha, Heather Job, and Olivia Hess. 2025. Autolabs: Cognitive multi-agent systems with self-correction for autonomous chemical experimentation. *arXiv preprint arXiv:2509.25651* (2025).

[53] Dmitrii Pantiukhin, Boris Shapkin, Ivan Kuznetsov, Antonia Anna Jost, Thomas Jung, and Nikolay Koldunov. 2025. PANGAEA GPT: A Coordinated Multi-Agent Architecture for Earth System Data Discovery and Analysis. In *EGU General Assembly Conference Abstracts*. EGU25–13656.

[54] Xin Peng, Zhengxun Lai, He Shao, Yi Shen, You Meng, and Johnny C Ho. 2025. Halide Perovskite Nanostructures: Processing Methods and Optoelectronics Applications. *npj Nanophotonics* 2, 1 (2025), 42.

[55] Yuanhao Qu, Kaixuan Huang, Ming Yin, Kanghong Zhan, Dyllan Liu, Di Yin, Henry C Cousins, William A Johnson, Xiaotong Wang, Mihir Shah, et al. 2025. CRISPR-GPT for agentic automation of gene-editing experiments. *Nature Biomedical Engineering* (2025), 1–14.

[56] Wissam A Saidi, Waseem Shadid, and Ivano E Castelli. 2020. Machine-learning structural and electronic properties of metal halide perovskites using a hierarchical convolutional neural network. *npj Computational Materials* 6, 1 (2020), 36.

[57] Timo Schick, Jane Dwivedi-Yu, Roberto Dess'i, Roberta Raileanu, Maria Lomeli, Eric Hambro, Luke Zettlemoyer, Nicola Cancedda, and Thomas Scialom. 2023. Toolformer: Language models can teach themselves to use tools. *Advances in Neural Information Processing Systems* 36 (2023), 68539–68551.

[58] Minjie Shen, Yanshu Li, Lulu Chen, and Qikai Yang. 2025. From mind to machine: The rise of manus ai as a fully autonomous digital agent. *arXiv preprint arXiv:2505.02024* (2025).

[59] Tao Song, Man Luo, Xiaolong Zhang, Linjiang Chen, Yan Huang, Jiaqi Cao, Qing Zhu, Daobin Liu, Baicheng Zhang, Gang Zou, et al. 2025. A multiagent-driven robotic ai chemist enabling autonomous chemical research on demand. *Journal of the American Chemical Society* 147, 15 (2025), 12534–12545.

[60] Zhilong Song, Shuaihua Lu, Minggang Ju, Qionghua Zhou, and Jinlan Wang. 2025. Accurate prediction of synthesizability and precursors of 3D crystal structures via large language models. *Nature Communications* 16, 1 (2025), 6530.

[61] Michael Soprano, Kevin Roitero, David La Barbera, Davide Ceolin, Damiano Spina, Gianluca Demartini, and Stefano Mizzaro. 2024. Cognitive biases in fact-checking and their countermeasures: A review. *Information Processing & Management* 61, 3 (2024), 103672.

[62] Kyle Swanson, Wesley Wu, Nash L Bulaong, John E Pak, and James Zou. 2025. The Virtual Lab of AI agents designs new SARS-CoV-2 nanobodies. *Nature* 646, 8085 (2025), 716–723.

[63] Qiuiling Tao, Pengcheng Xu, Minjie Li, and Wencong Lu. 2021. Machine learning for perovskite materials design and discovery. *Npj computational materials* 7, 1 (2021), 23.

[64] Shuxia Tao, Ines Schmidt, Geert Brocks, Junke Jiang, Ionut Tranca, Klaus Meerholz, and Selina Olthof. 2019. Absolute energy level positions in tin-and lead-based halide perovskites. *Nature communications* 10, 1 (2019), 2560.

[65] Ayseg"ul Toprak. 2025. High-accuracy machine learning approach for predicting J-V characteristics of perovskite solar cells under variable irradiance. *Scientific Reports* 15, 1 (2025), 41304.

[66] Agnes Valencia, Fei Liu, Xiangyang Zhang, Xiangkun Bo, Weilu Li, and Walid A Daoud. 2025. Auto-generating a database on the fabrication details of perovskite solar devices. *Scientific data* 12, 1 (2025), 270.

[67] Rens Van De Schoot, Jonathan De Bruin, Raoul Schram, Parisa Zahedi, Jan De Boer, Felix Weijdem, Bianca Kramer, Martijn Huijts, Maarten Hoogerwerf, Gerbrich Ferdinand, et al. 2021. An open source machine learning framework for efficient and transparent systematic reviews. *Nature machine intelligence* 3, 2 (2021), 125–133.

[68] Yuwei Wan, Tong Xie, Nan Wu, Wenjie Zhang, Chunyu Kit, and Bram Hoex. 2024. From tokens to materials: Leveraging language models for scientific discovery. *arXiv preprint arXiv:2410.16165* (2024).

[69] Hanchen Wang, Tianfan Fu, Yuanqi Du, Wenhao Gao, Kexin Huang, Ziming Liu, Payal Chandak, Shengchao Liu, Peter Van Katwyk, Andreea Deac, et al. 2023. Scientific discovery in the age of artificial intelligence. *Nature* 620, 7972 (2023), 47–60.

[70] Xin-De Wang, Zhi-Rui Chen, Peng-Jie Guo, Ze-Feng Gao, Cheng Mu, and Zhong-Yi Lu. 2025. Perovskite-R1: A Domain-Specialized LLM for Intelligent Discovery of Precursor Additives and Experimental Design. *arXiv preprint arXiv:2507.16307* (2025).

[71] Yidi Wang, Dan Sun, Bei Zhao, Tianyu Zhu, Chengcheng Liu, Zixuan Xu, Tianhang Zhou, and Chunming Xu. 2025. Data-Driven Perovskite Design via High-Throughput Simulation and Machine Learning. *Processes* 13, 10 (2025), 3049.

[72] Yue Wang, Senyue Ye, Jia Wei Melvin Lim, David Giovanni, Minjun Feng, Jianhui Fu, Harish NS Krishnamoorthy, Qianann Zhang, Qiang Xu, Rui Cai, et al. 2023. Carrier multiplication in perovskite solar cells with internal quantum efficiency exceeding 100%. *Nature Communications* 14, 1 (2023), 6293.

[73] Hasitha C Weerasinghe, Nasiruddin Macadam, Jueng-Eun Kim, Luke J Sutherland, Dechan Angmo, Leonard WT Ng, Andrew D Scully, Fiona Glenn, Regine Chantler, Nathan L Chang, et al. 2024. The first demonstration of entirely roll-to-roll fabricated perovskite solar cell modules under ambient room conditions. *Nature Communications* 15, 1 (2024), 1656.

[74] Jason Wei, Xuezhi Wang, Dale Schuurmans, Maarten Bosma, Fei Xia, Ed Chi, Quoc V Le, Denny Zhou, et al. 2022. Chain-of-thought prompting elicits reasoning in large language models. *Advances in neural information processing systems* 35 (2022), 24824–24837.

[75] Luyan Wu, Shuaifeng Hu, Feng Yang, Guixiang Li, Junke Wang, Weiwei Zuo, José J Jerónimo-Rendon, Silver-Hamill Turren-Cruz, Michele Saba, Michael Saliba, et al. 2025. Resilience pathways for halide perovskite photovoltaics under temperature cycling. *Nature Reviews Materials* (2025), 1–14.

[76] Yilei Wu, Chang-Feng Wang, Ming-Gang Ju, Qiangqiang Jia, Qionghua Zhou, Shuaihua Lu, Xinying Gao, Yi Zhang, and Jinlan Wang. 2024. Universal machine learning aided synthesis approach of two-dimensional perovskites in a typical laboratory. *Nature Communications* 15, 1 (2024), 138.

[77] Zonghan Wu, Shirui Pan, Fengwen Chen, Guodong Long, Chengqi Zhang, and Philip S Yu. 2020. A comprehensive survey on graph neural networks. *IEEE transactions on neural networks and learning systems* 32, 1 (2020), 4–24.

[78] Tian Xie and Jeffrey C Grossman. 2018. Crystal graph convolutional neural networks for an accurate and interpretable prediction of material properties. *Physical review letters* 120, 14 (2018), 145301.

[79] Pengcheng Xu, Yingying Ma, Wencong Lu, Minjie Li, Wenyue Zhao, and Zhilong Dai. 2025. Multi-objective optimization in machine learning assisted materials design and discovery. *Journal of Materials Informatics* 5, 2 (2025), N–A.

[80] Shaowen Xu, Jiehao He, Xiaoyan Liu, Yufeng Shan, and Ning Dai. [n. d.]. Machine-Learning-Assisted Optimization of Power Conversion Efficiency in Perovskite Solar Cells. *Available at SSRN 6079664* ([n. d.]).

[81] Shengxiang Xu, Jiayi Zhang, Shimin Di, Yuyu Luo, Liang Yao, Hanmo Liu, Jia Zhu, Fan Liu, and Min-Ling Zhang. 2025. Robustflow: Towards robust agentic workflow generation. *arXiv preprint arXiv:2509.21834* (2025).

[82] Hui Yang, Sifu Yu, and Yunzhong He. 2023. Auto-gpt for online decision making: Benchmarks and additional opinions. *arXiv preprint arXiv:2306.02224* (2023).

[83] Meifang Yang, Tian Tian, Yuxuan Fang, Wen-Guang Li, Gengling Liu, Wenhui Feng, Mingyi Xu, and Wu-Qiang Wu. 2023. Reducing lead toxicity of perovskite solar cells with a built-in supramolecular complex. *Nature Sustainability* 6, 11 (2023), 1455–1464.

[84] Claudio Zeni, Robert Pinsky, Daniel Zügner, Andrew Fowler, Matthew Horton, Xiang Fu, Zilong Wang, Aliaksandra Shysheya, Jonathan Crabbé, Shoko Ueda, et al. 2025. A generative model for inorganic materials design. *Nature* 639, 8055 (2025), 624–632.

[85] Jiyun Zhang, Jens A Hauch, and Christoph J Brabec. 2024. Toward self-driven autonomous material and device acceleration platforms (AMADAP) for emerging photovoltaics technologies. *Accounts of chemical research* 57, 9 (2024), 1434–1445.

[86] Xiaochun Zhang, Qing Cao, Luyao Wang, Tiankai Zhang, Kaiyu X Fu, Zhe Li, Antonio Abate, Meng Li, and Guixiang Li. 2025. Defect-Healing in Perovskite Photovoltaics Driving Long-Term Reliability and Performance. *Advanced Functional Materials* (2025), e23417.

[87] Yanbo Zhang, Sumeer A Khan, Adnan Mahmud, Huck Yang, Alexander Lavin, Michael Levin, Jeremy Frey, Jared Dunnmon, James Evans, Alan Bundy, et al. 2025. Exploring the role of large language models in the scientific method: from hypothesis to discovery. *npj Artificial Intelligence* 1, 1 (2025), 14.

[88] Jinbo Zhao, Zhenhuang Su, Jorge Pascual, Hongzhuo Wu, Haibin Wang, Mahmoud H Aldamasy, Zhengji Zhou, Chenyue Wang, Guixiang Li, Zhe Li, et al.

2024. Suppressed Defects by Functional Thermally Cross-Linked Fullerene for High-Efficiency Tin-Lead Perovskite Solar Cells. *Advanced Materials* 36, 36 (2024), 2406246.

[89] Yicheng Zhao, Jiyun Zhang, Zhengwei Xu, Shijing Sun, Stefan Langner, Noor Titan Putri Hartono, Thomas Heumueller, Yi Hou, Jack Elia, Ning Li, et al. 2021. Discovery of temperature-induced stability reversal in perovskites using high-throughput robotic learning. *Nature communications* 12, 1 (2021), 2191.

[90] Zhi-Hua Zhou and Ji Feng. 2019. Deep forest. *National science review* 6, 1 (2019), 74–86.

[91] Hongwei Zhu, Sam Teale, Muhammad Naufal Lintangpradipto, Suhas Mahesh, Bin Chen, Michael D McGehee, Edward H Sargent, and Osman M Bakr. 2023. Long-term operating stability in perovskite photovoltaics. *Nature Reviews Materials* 8, 9 (2023), 569–586.

## A Toolchain Construction

### A.1 Training Dataset Preparation

All datasets used in PeroMAS are derived from the **Perovskite Database Project** [21], an open-access database containing 43,398 experimental perovskite solar cell records across 410 attributes. These records span composition, fabrication process, device architecture, photovoltaic performance, and stability measurements. We processed this database into specialized sub-datasets tailored for distinct downstream tasks, as summarized in Table 3.

**Data Processing Pipeline.** Starting from the raw database, we applied a rigorous preprocessing workflow:

- (1) **Composition Filtering:** We retained only entries with valid perovskite compositions containing proper stoichiometric coefficients and recognized B-site metals (Pb, Sn, Bi, etc.).
- (2) **Attribute Cleaning:** Ambiguous or missing values in critical fields—such as solvent systems, deposition methods, and additive descriptions—were standardized or removed.
- (3) **Stratified Deduplication:** To balance the dataset, we performed deduplication while preserving the diversity of synthesis methods, ensuring that unique process-property mappings were retained.
- (4) **Structure Augmentation:** We queried Materials Project [22] API to enrich the dataset with crystal structures (CIF) and DFT-calculated properties (e.g., band gap, energy above hull) for matched compositions (achieving a 75.2% match rate).

**Table 3: Overview of task-specific datasets constructed for PeroMAS. The data is categorized by the functional module it supports.**

Task / Functional Module	Split (Train / Val)	Total Size
<b>1. Synthesis Feasibility Assessment</b>		
Positive Samples (Synthesizable)	2,608 / 290	2,898
Negative Samples (Non-synthesizable)	—	700
<b>2. Synthesis Route Planning</b>		
Method Recommendation	4,500 / 500	5,000
Precursor Identification	—	2,296
<b>3. Crystal Structure Generation</b>		
Core Set (Unique Compositions)	639 / 72	711
Expanded Set (Data Augmentation)	37,296 / 4,145	41,441
<b>4. Property Prediction</b>		
Multi-target Regression	~569 / 142	711

Table 4 details the specific physical attributes extracted to support these tasks.

### A.2 MCP Tool

To standardize the interaction between agents and external knowledge, we encapsulated specialized algorithms and data sources into the Model Context Protocol (MCP). Table 5 details the core toolset assigned to each functional agent.

**Table 4: Key attributes extracted from the Perovskite Database.**

Category	Attributes
Composition	A/B/X-site ions, stoichiometric coefficients
Performance	PCE, $V_{oc}$ , $J_{sc}$ , Fill Factor (FF)
Band gap	Experimental & DFT-calculated values
Fabrication	Deposition method, solvent system, annealing temp.
Structure	CIF files (augmented via Materials Project)
Stability	T80 lifetime, PCE retention rate
Device	Device architecture (n-i-p / p-i-n), layer thickness

**Table 5: List of specialized MCP tools employed by PeroMAS. Citations indicate the underlying algorithms or data sources.**

Target Agent	MCP Tool ID	Backend / Description
Miner	arxiv-mcp	Real-time literature retrieval via arXiv API
	Sci-mcp	Cross-database search (ScienceDirect, Springer)
	extract-mcp	Hybrid information extraction engine integrating LLM [68] and SciBERT [3]
Designer	MatterGen	Generative model for crystal structure inverse design [84]
	CSLLM	Synthesis feasibility reasoning and recipe recommendation [60]
	MatProj-mcp	Structure and property querying via Materials Project API [22]
Emulator	CGCNN	Graph neural network for bandgap and formation energy prediction [78]
	Pero-ML	Data-driven regression models (XG-Boost,RF,NN) [20] for device performance (PCE, $V_{oc}$ )
Analyst	SHAP-mcp	Interpretable machine learning analysis for feature attribution [42]
	Pymatgen	Geometric analysis and structure manipulation toolkit [51]
	ASE	Atomic Simulation Environment for thermodynamic checks [17]

### A.3 Hardware Specifications

We deploy the full-chain MCP tool training and runtime environment on a high-performance computing cluster equipped with 4× NVIDIA H100 GPUs.

## B Dry-Lab Case

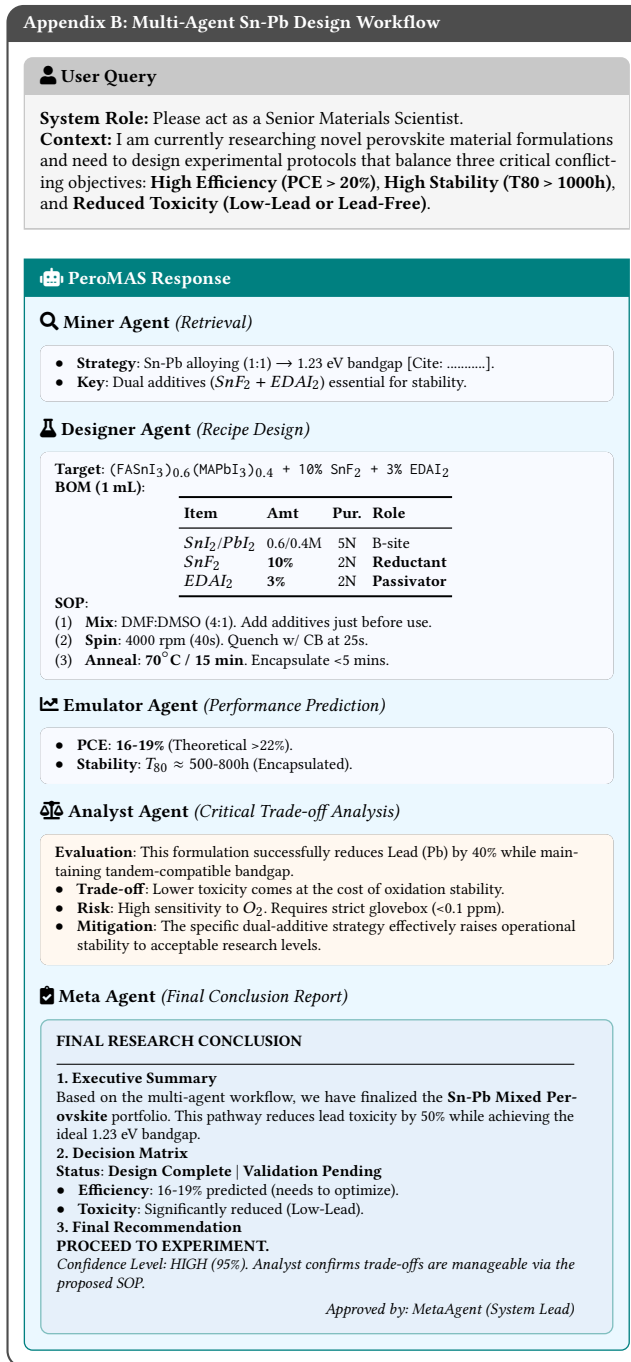


Figure 7: Complete PeroMAS workflow.

## C Wet-Lab Fabrication Details

All physical validation experiments were conducted in a standard-ized ISO Class 7 cleanroom environment. The specific fabrication

protocol for the p-i-n inverted perovskite solar cells includes three key stages:

**Substrate Preparation & HTL.** Indium Tin Oxide (ITO) glass substrates ( $15\ \Omega/\text{sq}$ ) were sequentially cleaned via ultrasonication in detergent, deionized water, acetone, and isopropanol for 20 minutes each. After drying, the substrates underwent UV-Ozone treatment for 15 minutes to improve wettability. A Nickel Oxide ( $\text{NiO}_x$ ) nanoparticle dispersion was then spin-coated at 4000 rpm for 30s and annealed at 150°C for 30 minutes in ambient air to form the hole transport layer.

**Perovskite Deposition.** The substrates were transferred to a nitrogen-filled glovebox ( $O_2 < 0.1\ \text{ppm}$ ,  $H_2O < 0.1\ \text{ppm}$ ). The perovskite precursor solution, prepared according to the exact stoichiometry output by the Designer Agent, was spin-coated using a one-step method. The specific spin program typically involved 1000 rpm for 10s and 4000 rpm for 30s, with anti-solvent (chlorobenzene) dropped 10s prior to the end. The films were subsequently annealed at 100°C for 10–60 minutes (depending on the agent's recipe) to promote crystallization.

**ETL & Electrode Evaporation.** Finally, the Electron Transport Layer (ETL) consisting of  $C_{60}$  (20 nm) and Bathocuproine (BCP, 5 nm), followed by a Silver (Ag) electrode (100 nm), were sequentially deposited via thermal evaporation under a high vacuum of  $5 \times 10^{-4}\ \text{Pa}$ . The active area of each device was defined as  $0.09\ \text{cm}^2$  using a metal shadow mask.

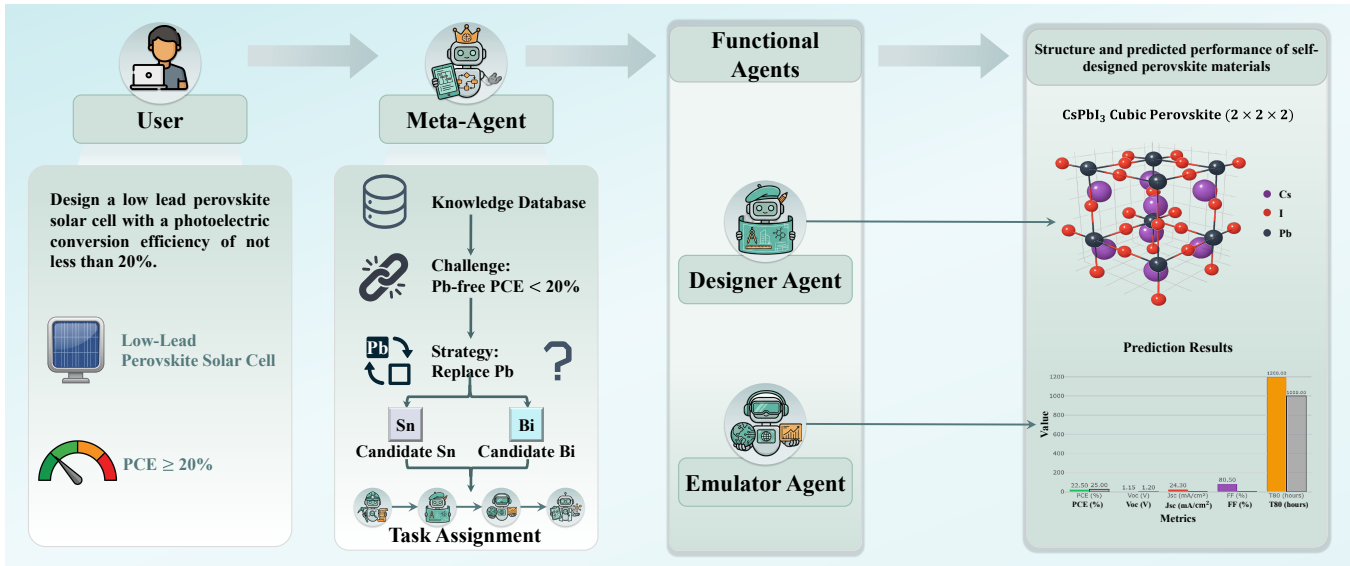


Figure 8: Case of dry-lab experiments designed by PeroMAS.